RSC Advances

PAPER

View Article Online
View Journal | View Issue

Cite this: *RSC Adv.*, 2019, **9**, 4665

Stable global tubular boron clusters in Na_2B_{18} and $Na_2B_{18}^-$†

Xue Dong,[a] Anita Das,[b] Wei-yan Liang,[a] Meng-hui Wang[a] and Zhong-hua Cui *[a]

Received 10th December 2018
Accepted 28th January 2019

DOI: 10.1039/c8ra10123j

rsc.li/rsc-advances

The electron deficiency and strong bonding capacity of boron have created numerous species with unusual structural and electronic properties in the form of pure and hetero-atom doped boron clusters. Here we identified D_{9d}-symmetry Na_2B_{18} and $Na_2B_{18}^-$ tubular boron clusters as global minima, whose stability is significantly enhanced by two doped sodium atoms. The doped Na atoms trigger strong charge transfer from Na to the boron motifs, resulting in salt complexes ($Na_2^{2+}B_{18}^{2-}$ and $Na_2^{2+}B_{18}^{3-}$). In particular, the optimal electrostatic interactions arising from the doping effect play a crucial role in stabilizing the tubular structure against the planar and quasi-planar preferences of the negatively charged boron clusters.

1. Introduction

Zero-dimensional boron clusters have received incessant attention from the aspects of their molecular shapes and multi-center bonding.[1,2] In comparison with cage-like structured bulk boron,[3] boron clusters B_n, from small size to an extended size range at least up to B_{38}^- (B_{16}^+), prefer to form planar or quasi-planar structures, which have been confirmed *via* experimental and high-level computational studies.[4,5] Remarkably, over past decades, a set of pure and doped boron clusters have been systematically characterized, which constantly pushes our current understanding of the structural evolution of isolated boron clusters.[6–8] Recently, the discovery of all-boron fullerenes,[9,10] borophenes and boron sheets on metal surfaces,[11–14] motivated by their carbon analogues, has overwhelmingly enriched studies of the chemistry of boron and may lead to new boron-based materials. On the other hand, studies of doped boron clusters with transition metals, such as metal-centered monocyclic rings,[7] metalloborophenes,[15] half-sandwich structures,[16,17] and metal-centered tubular structures and cages,[18–23] have created a series of clusters with novel structures and chemical bonding. All these doped-boron clusters have pushed the limits of recorded coordination numbers and structural chemistry.

Tubular boron structures are a very special case in terms of isolated boron clusters. They have aroused widespread interest for many years because they can be considered not only as a key indicator of the 2D-to-3D (planar to three-dimensional form) structural transition of boron clusters, but also as embryos for boron nanotubes. The two-ring B_{20} tubular cluster is the first example and it is characterized as the global minimum on the basis of computational calculations, yet it has not been observed experimentally.[24,25] Remarkably, cationic B_{2n}^+ ($n = 9$–10) tubular structures were clearly confirmed *via* joint ion mobility experiments combined with density functional theory (DFT) calculations.[5] For anionic boron clusters, planar or quasi-planar boron (2D) forms remain critical competing alternatives that are more stable in energy than the tubular forms; this has been confirmed *via* photoelectron spectroscopy (PES) combined with theoretical investigations.[26–28] The 2D preference of negatively charged boron clusters can be ascribed to the fact that electron addition tends to enhance the stability of the 2D form over the corresponding 3D isomer, irrespective of the available electrons.[29] For instance, as shown in Scheme 1, the tubular

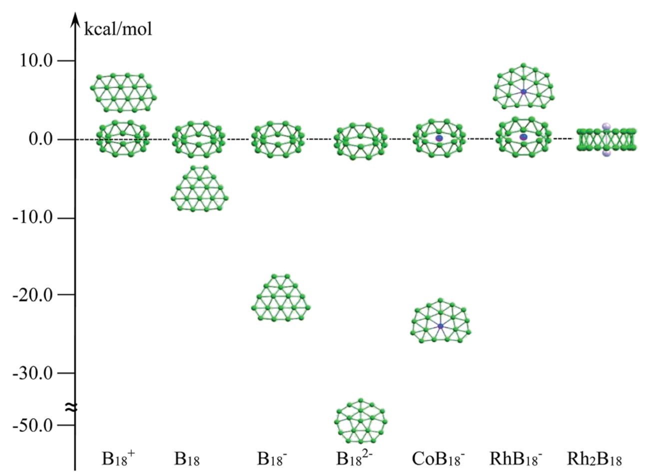

Scheme 1 The relative energy differences in kcal mol^{-1} between tubular structures and low-lying planar forms at the DFT level.[5,30–32]

[a]Institute of Atomic and Molecular Physics, Jilin Provincial Key Laboratory of Applied Atomic and Molecular Spectroscopy, Jilin University, Changchun, China. E-mail: zcui@jlu.edu.cn

[b]Department of Chemistry, Indian Institute of Engineering Science and Technology, Shibpur, Howrah, India

† Electronic supplementary information (ESI) available. See DOI: 10.1039/c8ra10123j

structure of B_{18}^{+} was suggested to be the global minimum, whereas the B_{18}, B_{18}^{-} and B_{18}^{2-} analogues were found to be high-energy isomers.[5,30–32] Meanwhile, it is noted that the stability of a tubular structure deceases along with an increase in electrons, so it is difficult to stabilize doubly or more negatively charged boron tubular clusters. Interestingly, doped boron clusters with transition metals have led to the achievement of mono-metal-centered tubular boron clusters. Recently, tubular MB_{16}^{-} (M = Co, Mn), RhB_{18}^{-} and TaB_{20}^{-} have been characterized *via* PES combined with theoretical predictions.[18,22,33,34] Clearly, the strong covalent interactions between the transition metal and tubular boron motifs significantly stabilize the tubular structures. Recent works have shown that the tubular-to-cage-like structural transition has started in large mono-metal-based boron clusters.[21,35]

Our recent work revealed that the thermodynamic stability of tubular boron clusters was significantly promoted in Li-doped boron species (LiB_{20} and LiB_{20}^{-}) in comparison with bare anionic B_{20} species.[36] This is because the optimal electrostatic interactions arising from charge transfer significantly improve the stability of tubular boron clusters. In this work, we followed the same strategy and found that the effects from two doped Na atoms can tune the preference between 2D and tubular forms in the difficult case of negatively charged B_{18}, where the tubular form is a high-energy isomer. Herein we report an investigation into di-alkali metal doped boron clusters in the form of Na_2B_{18} and $Na_2B_{18}^{-}$ species. Surprisingly, rather than forming a half-sandwich structure with the quasi-planar structure of bare B_{18}, B_{18}^{-} and B_{18}^{2-}, the Na_2B_{18} and $Na_2B_{18}^{-}$ clusters are predicted to have tubular structures, where the two Na atoms are located on the high-symmetry axis of the tubular structures and the two sides of the double-ring boron. Chemical bonding analysis has revealed that the tubular clusters are charge-transfer complexes formed by Na^{+} and B_{18}^{2-} (B_{18}^{3-}), where the optimal electrostatic interactions between Na and boron clusters are found.

2. Computational details

The structure search is performed using the PSO algorithm within the revolutionary scheme, as implemented *via* CALYPSO (Crystal structure AnaLYsis by Particle Swarm Optimization) code.[37] Specifically, in the PSO search, the population size is set to 30, and the number of generations is maintained at 30. The best 60% of structures are selected through PSO to generate the next generation, while the other structures are generated randomly to guarantee structural diversity. The B3LYP/6-31G(d) level of theory was used to optimize the initial structure with a variety of spin states, and for the low-lying (<30 kcal mol^{-1} above the global minimum) isomers, we employed B3LYP/6-311+G(d) and TPSSh/6-311+G(d) for better geometrical and frequency predictions. The single-point calculations for the low-lying isomers were performed at the CCSD(T)/6-311+G(d)//TPSSh/6-311+G(d) level of theory. We found that T1 values are in the range of 0.01 to 0.03 for the low-lying isomers, indicating that the mono-determinantal method can be safely employed for our species. Electron detachment energies from the closed-shell ground state of $Na_2B_{18}^{-}$ and the low-lying isomers were computed at the TD-B3LYP/6-311+G(2df) level of theory based on B3LYP/6-311+G(d) geometry. The chemical bonding in Na_2B_{18} and $Na_2B_{18}^{-}$ has been revealed *via* natural bonding orbital (NBO)[38] and adaptive natural density partitioning (AdNDP) algorithm analysis.[39] Total energies were corrected using the zero-point energies (ZPE). All calculations were carried out with the GAUSSIAN09 program package.[40]

3. Results and discussion

CALYPSO was performed to explore the potential energy surfaces of neutral Na_2B_{18} and anionic $Na_2B_{18}^{-}$ clusters in low and high spin states. At the B3LYP/6-311+G(d) and TPSSh/6-311+G(d) levels of theory, the tubular structures of Na_2B_{18} and $Na_2B_{18}^{-}$ were found to be local minima, with large lowest frequencies of above 100.0 cm^{-1} (see Table 1) and high D_{9d}-symmetry, where the two Na atoms are located on the high-symmetry axis of the tubular structures (see Fig. 1). Furthermore, the tubular structures were predicted to be global minima at the B3LYP, TPSSh and single-point CCSD(T) levels of theory with the 6-311+G(d) basis set. In particular, they are 2.1 and 2.0 kcal mol^{-1} more stable than the second lowest isomers of the Na_2B_{18} and $Na_2B_{18}^{-}$ species, respectively, at the single-point CCSD(T)/6-311+G(d)//TPSSh/6-311+G(d) level of theory. All low-lying isomers are provided in the ESI.† For the nearest competing isomers, the B_{18} motif possesses a quasi-planar structure that is similar to the low-lying isomers of bare anionic B_{18}^{2-}, and the two Na atoms were located above or beside the quasi-plane of the boron clusters.

The structural details of the tubular structures of Na_2B_{18} and $Na_2B_{18}^{-}$ are tabulated in Table 1. The structures of the neutral and anionic forms are very similar, except for the significant difference in the Na–B and Na–Na interaction distances. Contrasting with neutral Na_2B_{18}, the Na–B and Na–Na interaction distances in the $Na_2B_{18}^{-}$ cluster were clearly reduced by 0.06 and 0.17 Å, respectively. The calculated natural atomic charge on the Na atom is about 0.95 $|e|$ in the Na_2B_{18} and $Na_2B_{18}^{-}$ species, indicating that Na serves as the donor of one electron to the B_{18} tubular motifs, forming typical charge-transfer $Na_2^{2+}B_{18}^{2-}$ and $Na_2^{2+}B_{18}^{3-}$ complexes. The calculated natural atomic charges on the B atoms are −0.11 and −0.16 $|e|$ in the Na_2B_{18} and $Na_2B_{18}^{-}$ species, respectively, resulting in stronger electrostatic interactions between Na^{+} and the anionic boron cluster in the $Na_2B_{18}^{-}$ system compared to the neutral analogue. This is the reason that shorter Na–B and Na–Na interaction distances were found in the anionic $Na_2B_{18}^{-}$ system. It is worth noting that the Na–B bond distances in both neutral and anionic Na_2B_{18} are longer than a Na–B single bond (2.4 Å) obtained using the self-consistent covalent radii of Pyykko,[41] which is consistent with the negligible Wiberg bond indices (WBIs) listed in Table 1. Clearly, the two kinds of B–B bonds, inter-ring and intra-ring, are found in both neutral and anionic tubular species. The inter-ring B–B bonds are responsible for holding two monocyclic B_9 rings together, and are clearly longer (about 0.07 Å) than the intra-ring B–B bonds (1.62 Å). The WBIs of the two kinds of B–B bonds further confirm the assessment of

Table 1 The smallest frequencies (V_{min}, cm^{-1}) of the tubular structures, NPA charges on Na and B (Q_{Na} and Q_B, |e|), bond properties (bond length (Å), Wiberg bond indices in parenthesis) and HOMO–LUMO gaps (gap, eV). All values have been computed at the B3LYP/6-311+G(d) level of theory

Species	V_{min} (cm^{-1})	B_{Na-Na} (Å)	B_{Na-B} (Å)	B_{B-B} (Å)	Q_{Na} (|e|)	Q_B (|e|)	Gap (eV)
Na_2B_{18}	131.3	4.501 (0.00)	2.810 (0.01)	1.688; 1.619 (0.71); (0.96)	0.96	−0.11	2.07
$Na_2B_{18}^-$	176.1	4.329 (0.00)	2.751 (0.01)	1.713; 1.615 (0.65); (1.01)	0.95	−0.16	1.15

bond distances. Moreover, their strength can be referenced to the value of a typical B–B single bond (1.70 Å). It is worthy of note that two such kinds of B–B bonds have been found in all the tubular structures of pure boron or hetero-doped boron clusters. Note that the formation of Na–B interactions in Na_2B_{18} and $Na_2B_{18}^-$ species effectively removes the electronic charge of two Na atoms, which evidently promotes the electrostatic interactions between Na^+ and the tubular boron motifs, giving rise to the eighteen optimal Na–B interactions and high thermodynamic stability of the tubular structures.

As discussed above, both Na_2B_{18} and $Na_2B_{18}^-$ species are essentially charge-transfer complexes between Na^+ and B_{18}^{2-} (B_{18}^{3-}). To discover how the further thermodynamic stability of tubular structures is gained, we investigated two kinds of dissociation pathways by means of: (i) $Na_2B_{18} \rightarrow 2Na^+ + B_{18}^{2-}$ and (ii) $Na_2B_{18} \rightarrow 2Na + B_{18}$; and (iii) $Na_2B_{18}^- \rightarrow 2Na^+ + B_{18}^{3-}$ and (iv) $Na_2B_{18}^- \rightarrow 2Na + B_{18}^-$ for the Na_2B_{18} and $Na_2B_{18}^-$ species, where all these fragments are in their electronic ground states. At the TPSSh/6-311+G(d) level of theory, pathways (i) and (ii) for Na_2B_{18} give dissociation energies of 283.1 and 121.7 kcal mol^{-1}, respectively, and pathways (iii) and (iv) for $Na_2B_{18}^-$ give dissociation energies of 441.4 and 81.5 kcal mol^{-1}, respectively. The high dissociation energies indicate the good stability against the dissociation of M and M^+ for tubular motifs. Additionally, the degrees of Na^+ and tubular boron interaction could be approximately estimated and compared. The interaction energies between Na^+ and tubular boron are estimated to be 171.5 and 253.9 kcal mol^{-1}, half of the total dissociation energies of pathways (i) and (iii), respectively, where the boron fragments are in ground electronic states with the framework of a tubular structure. Strong electrostatic interactions between Na^+ and the tubular boron motifs provide a key driving force for stabilizing these charge-transfer complexes in the neutral and anionic states. The optimized structures of the bare tubular B_{18}^{2-} and B_{18}^{3-} clusters lie 59.8 and 64.3 kcal mol^{-1} higher in energy, respectively, than the quasi-planar minimum at the TPSSh/6-311+G(d) level of theory. The tubular structures of the anionic B_{18}^{2-} and B_{18}^{3-} species are significantly stabilized by means of doping two cationic Na^+ ions, resulting in effective charge transfer in the tubular structures. Moreover, additional electrostatic stabilization occurred in $Na_2B_{18}^-$ compared to Na_2B_{18} *via* one more electron being only localized in the tubular boron motifs. Thus, only electrostatic interactions between Na and the B_{18} clusters make Na_2B_{18} and $Na_2B_{18}^-$ highly thermodynamically stable species.

The molecular orbitals of $Na_2B_{18}^-$ are given in Fig. S2,† and one unpaired electron resides in a singly occupied molecular orbital (SOMO) instead of a closed-shell neutral one. To further understand the structure and stability of the tubular structure, we analyzed the chemical bonding of the Na_2B_{18} system using the adaptive natural density partitioning (AdNDP) method at the B3LYP/6-311+G(d) level of theory. AdNDP analysis transformed the 28 canonical molecular orbitals of the Na_2B_{18} system into localized and delocalized multi-center bonds, as shown in Fig. 2. There are three types of bond in the tubular boron cluster. The first row depicts eighteen two center-two electron (2c–2e) localized σ bonds with an occupation number (ON) of 1.85 |e|, which is very similar to the ON of a bare B_{18} cluster, as shown in the ESI.† The remaining AdNDP bonds can be considered as delocalized multi-center σ and π bonds

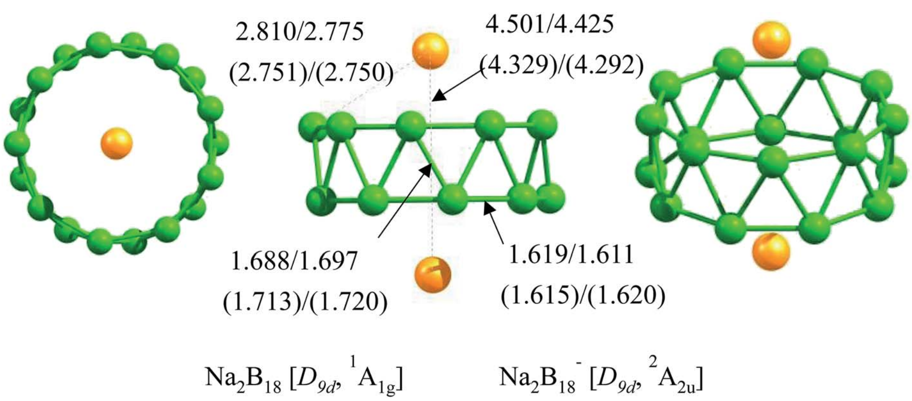

Fig. 1 Three views of the Na_2B_{18} and $Na_2B_{18}^-$ species. The point group symmetries and spectroscopic states are shown in square brackets. All distances are in Å; the values shown in parentheses refer to the anionic $Na_2B_{18}^-$ system, the values before the backslash are obtained at the B3LYP/6-311+G(d) level of theory and the ones after the backslash are obtained at the TPSSh/6-311+G(d) level of theory.

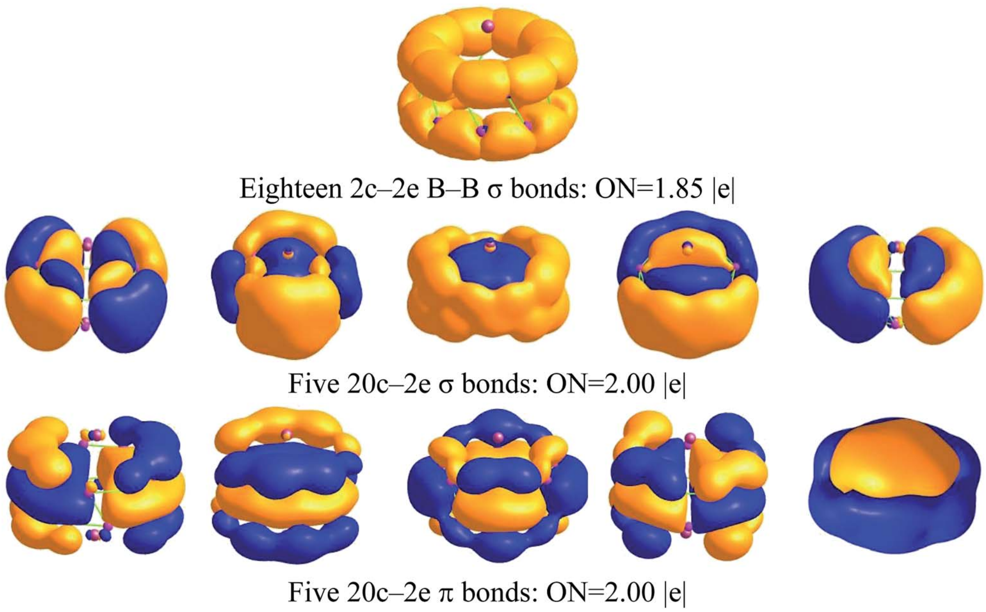

Fig. 2 AdNDP analysis of Na_2B_{18} computed at the B3LYP/6-311+G(d) level of theory; ON stands for occupation number.

between the two B_9 rings. The second and third rows exhibit five delocalized σ and π bonds, respectively, representing strong bonding interactions between the five delocalized σ and π bonds in each B_9 ring. The second and third row each describe an aromatic system, resulting in fairly stable D_{9d} tubular Na_2B_{18} clusters.

To facilitate the future experimental characterization of the anionic tubular $Na_2B_{18}^-$ system, we use time-dependent (TD)-B3LYP/6-311+G(2df) theory to calculate the vertical electron detachment energies (VDEs) for the three lowest energy isomers. Tubular $Na_2B_{18}^-$ is predicted to have an extremely low first VDE of 1.65 eV, originating from the detachment of the electron from the SOMO, which is significantly lower in energy than the other low-lying isomers by about 0.9 eV (see Table S1–S3†). The first adiabatic electron detachment energy (ADE) is calculated as the total energy difference between $Na_2B_{18}^-$ and Na_2B_{18} using their respective optimized geometries. The ADE values are 1.63, 1.97 and 1.88 eV for the three low-lying isomers I, II and III. Overall, the tubular structure has a clear signal compared to the other low-lying isomers and this can be distinguished in experiments. The calculated infrared (IR) absorption spectrum of the neutral Na_2B_{18} tubular structure is depicted in Fig. S5,† which should aid the forthcoming experimental characterization of the tubular structures.

Small boron clusters have been found to show planar and quasi-planar preferences and electron delocalization in both the σ and π frameworks has been shown to be the major driving force. A tubular structure was first shown to be viable for the neutral B_{20} cluster and was suggested to be the embryo for boron nanotubes.[24] Ion mobility and DFT calculations suggested that cationic boron clusters (B_n^+) prefer to take up tubular structures for $n > 15$.[5] However, for anionic B_n^- clusters, no tubular clusters have been observed up to $n = 40$.[4] This trend results from the fact that electron addition tends to enhance the stability of 2D isomers over the corresponding 3D isomers, irrespective of the available electrons. Clearly, the strong metal–boron covalent interactions in CoB_{16}^-, MnB_{16}^- and RhB_{18}^- are critical in stabilizing tubular structures, and they require a perfect electronic and structural match between the metal and the boron cluster to justify the balance between M–B interactions in the tubular isomers and 2D electron delocalization.[18,33,34] By means of a detailed analysis of the structural and electronic properties, the anionic tubular structures stabilized by doped alkali metals are found to be due to strong electrostatic interactions between Na^+ and the anionic B_{18} motifs. Following this idea, we further extend this strategy to the other alkali metals (M = Li, K). The initial geometries were constructed by replacing Na with M atoms in term of the isomers of the Na-doped system, as shown in Fig. S1 and S2.† As shown in Fig. S6,† all the low-lying isomers are given for the M_2B_{18} and $M_2B_{18}^-$ (M = Li, K) species. As predicted, the tubular boron clusters were the lowest-energy isomers for all species at the TPSSh/6-311+G(d) level of theory. In the case of tubular boron structures, two kinds of B–B bond show an insignificant change for all the M-doped systems (M = Li, Na, K), whereas the M–B and M–M interaction distances increase along with the size of the alkali metal (see Fig. S7†). This work suggests a new strategy where the electrostatic interactions can be used to clearly tune the boron arrangement preference, which is further useful for understanding the structural evolution of boron clusters.

4. Conclusions

In summary, we present a symmetric theoretical investigation into the viability of tubular structures in Na_2B_{18} and $Na_2B_{18}^-$ clusters. We found that tubular structures with high D_{9d} symmetry have been predicted to be global minima *via* high-level calculations. Chemical bonding analysis revealed that the tubular structures are charge-transfer complexes, where the two Na atoms are localized on the axis of the tubular structure, giving rise to optimal Na–B electrostatic interactions. The strong electrostatic interactions between Na^+ atoms and tubular boron structures appear to be critical in stabilizing the tubular structure, which is an unfavorable configuration in comparison to the quasi-planar and planar arrangement of pure anionic boron species because of 2D electron delocalization. The Na_2B_{18} and $Na_2B_{18}^-$ species represent a new class of metal-doped boron clusters, providing new insights into tubular boron species and further recommending boron clusters as a promising building block for new boron-based nanostructures.

Conflicts of interest

There are no conflicts to declare.

Acknowledgements

This work was funded by the National Natural Science Foundation of China (No. 11874178, 21503088). Anita Das acknowledges SERB, India, for providing a National Post-Doctoral Fellowship (N-PDF application no. PDF/2017/000315). The partial calculations in this work were supported by the High Performance Computing Center of Jilin University, China.

References

1 T. Kondo, *Sci. Technol. Adv. Mater.*, 2017, **18**, 780–804.
2 L.-S. Wang, *Int. Rev. Phys. Chem.*, 2016, **35**, 69–142.
3 A. R. Oganov, J. Chen, C. Gatti, Y. Ma, Y. Ma, C. W. Glass, Z. Liu, T. Yu, O. O. Kurakevych and V. L. Solozhenko, *Nature*, 2009, **457**, 863–867.
4 W.-L. Li, X. Chen, T. Jian, T.-T. Chen, J. Li and L.-S. Wang, *Nat. Rev. Chem.*, 2017, **1**, 71.
5 E. Oger, N. R. M. Crawford, R. Kelting, P. Weis, M. M. Kappes and R. Ahlrichs, *Angew. Chem., Int. Ed.*, 2007, **46**, 8503–8506.
6 A. P. Sergeeva, I. A. Popov, Z. A. Piazza, W.-L. Li, C. Romanescu, L.-S. Wang and A. I. Boldyrev, *Acc. Chem. Res.*, 2014, **47**, 1349–1358.
7 C. Romanescu, T. R. Galeev, W.-L. Li, A. I. Boldyrev and L.-S. Wang, *Acc. Chem. Res.*, 2013, **46**, 350–358.
8 A. N. Alexandrova, A. I. Boldyrev, H. J. Zhai and L. S. Wang, *Coord. Chem. Rev.*, 2006, **250**, 2811–2866.
9 H.-J. Zhai, Y.-F. Zhao, W.-L. Li, Q. Chen, H. Bai, H.-S. Hu, Z. A. Piazza, W.-J. Tian, H.-G. Lu, Y.-B. Wu, Y.-W. Mu, G.-F. Wei, Z.-P. Liu, J. Li, S.-D. Li and L.-S. Wang, *Nat. Chem.*, 2014, **6**, 727–731.
10 J. Lv, Y. Wang, L. Zhu and Y. Ma, *Nanoscale*, 2014, **6**, 11692–11696.
11 W. L. Li, Q. Chen, W. J. Tian, H. Bai, Y. F. Zhao, H. S. Hu, J. Li, H. J. Zhai, S. D. Li and L. S. Wang, *J. Am. Chem. Soc.*, 2014, **136**, 12257–12260.
12 A. J. Mannix, X.-F. Zhou, B. Kiraly, J. D. Wood, D. Alducin, B. D. Myers, X. Liu, B. L. Fisher, U. Santiago, J. R. Guest, M. J. Yacaman, A. Ponce, A. R. Oganov, M. C. Hersam and N. P. Guisinger, *Science*, 2015, **350**, 1513–1516.
13 B. Feng, J. Zhang, Q. Zhong, W. Li, S. Li, H. Li, P. Cheng, S. Meng, L. Chen and K. Wu, *Nat. Chem.*, 2016, **8**, 563–568.
14 Z. Zhang, Y. Yang, E. S. Penev and B. I. Yakobson, *Adv. Funct. Mater.*, 2017, **27**, 1605059.
15 W.-L. Li, T. Jian, X. Chen, T.-T. Chen, G. V. Lopez, J. Li and L.-S. Wang, *Angew. Chem., Int. Ed.*, 2016, **55**, 7358–7363.
16 T.-T. Chen, W.-L. Li, T. Jian, X. Chen, J. Li and L.-S. Wang, *Angew. Chem., Int. Ed.*, 2017, **56**, 6916–6920.
17 I. A. Popov, W. Li, Z. A. Piazza, A. I. Boldyrev and L. Wang, *J. Phys. Chem. A*, 2014, **118**, 8098–8105.
18 I. a Popov, T. Jian, G. V Lopez, A. I. Boldyrev and L.-S. Wang, *Nat. Commun.*, 2015, **6**, 8654.
19 J. Lv, Y. Wang, L. Zhang, H. Lin, J. Zhao and Y. Ma, *Nanoscale*, 2015, **7**, 10482–10489.
20 N. M. Tam, H. T. Pham, L. Van Duong, M. P. Pham-Ho and M. T. Nguyen, *Phys. Chem. Chem. Phys.*, 2015, **17**, 3000–3003.
21 H.-R. Li, H. Liu, X.-X. Tian, W.-Y. Zan, Y.-W. Mu, H.-G. Lu, J. Li, Y.-K. Wang and S.-D. Li, *Phys. Chem. Chem. Phys.*, 2017, **19**, 27025–27030.
22 W.-L. Li, T. Jian, X. Chen, H.-R. Li, T.-T. Chen, X.-M. Luo, S.-D. Li, J. Li and L.-S. Wang, *Chem. Commun.*, 2017, **53**, 1587–1590.
23 Y. Wang, X. Wu and J. Zhao, *J. Cluster Sci.*, 2018, **29**, 847–852.
24 B. Kiran, S. Bulusu, H.-J. Zhai, S. Yoo, X. C. Zeng and L.-S. Wang, *Proc. Natl. Acad. Sci. U. S. A.*, 2005, **102**, 961–964.
25 C. Romanescu, D. J. Harding, A. Fielicke and L.-S. Wang, *J. Chem. Phys.*, 2012, **137**, 14317.
26 A. P. Sergeeva, Z. A. Piazza, C. Romanescu, W. L. Li, A. I. Boldyrev and L. S. Wang, *J. Am. Chem. Soc.*, 2012, **134**, 18065–18073.
27 I. A. Popov, Z. A. Piazza, W.-L. Li, L.-S. Wang and A. I. Boldyrev, *J. Chem. Phys.*, 2013, **139**, 144307.
28 X.-M. Luo, T. Jian, L.-J. Cheng, W.-L. Li, Q. Chen, R. Li, H.-J. Zhai, S.-D. Li, A. I. Boldyrev, J. Li and L.-S. Wang, *Chem. Phys. Lett.*, 2017, **683**, 336–341.
29 H. T. Pham, L. Van Duong, B. Q. Pham and M. T. Nguyen, *Chem. Phys. Lett.*, 2013, **577**, 32–37.
30 A. P. Sergeeva, B. B. Averkiev, H.-J. Zhai, A. I. Boldyrev and L.-S. Wang, *J. Chem. Phys.*, 2011, **134**, 224304.
31 D. Moreno, S. Pan, L. L. Zeonjuk, R. Islas, E. Osorio, G. Martínez-Guajardo, P. K. Chattaraj, T. Heine and G. Merino, *Chem. Commun.*, 2014, **50**, 8140–8143.
32 T. B. Tai, N. M. Tam and M. T. Nguyen, *Chem. Phys. Lett.*, 2012, **530**, 71–76.
33 T. Jian, W.-L. Li, I. A. Popov, G. V. Lopez, X. Chen, A. I. Boldyrev, J. Li and L.-S. Wang, *J. Chem. Phys.*, 2016, **144**, 154310.
34 T. Jian, W.-L. Li, X. Chen, T.-T. Chen, G. V. Lopez, J. Li and L.-S. Wang, *Chem. Sci.*, 2016, **7**, 7020–7027.
35 H.-R. Li, H. Liu, X.-Q. Lu, W.-Y. Zan, X.-X. Tian, H.-G. Lu, Y.-B. Wu, Y.-W. Mu and S.-D. Li, *Nanoscale*, 2018, **10**, 7451–7456.
36 W. Liang, A. Das, X. Dong and Z. Cui, *Phys. Chem. Chem. Phys.*, 2018, **20**, 16202–16208.
37 H. Wang, Y. Wang, J. Lv, Q. Li, L. Zhang and Y. Ma, *Comput. Mater. Sci.*, 2016, **112**, 406–415.

38 A. E. Reed, R. B. Weinstock and F. Weinhold, *J. Chem. Phys.*, 1985, **83**, 735–746.
39 D. Y. Zubarev and A. I. Boldyrev, *Phys. Chem. Chem. Phys.*, 2008, **10**, 5207–5217.
40 M. J. Frisch, G. W. Trucks, H. B. Schlegel, G. E. Scuseria, M. A. Robb, J. R. Cheeseman, G. Scalmani, V. Barone, B. Mennucci, G. A. Petersson, *et al.*, *Gaussian 09, Revision D.01*, Gaussian, Inc., Wallingford, CT, 2009.
41 P. Pyykko and M. Atsumi, *Chem.–Eur. J.*, 2009, **15**, 12770–12779.